Pergamon

Int. J. Heat Mass Transfer. Vol. 41, No. 11 pp. 1445–1458, 1998

Printed in Great Britain
0017–9310/98 $19.00+0.00

PII: S0017–9310(97)00258–5

Experimental study of unsteady thermal characteristics and rotation induced stabilization of air convection in a bottom heated rotating vertical cylinder

Y. T. KER, Y. H. LI and T. F. LIN†

Department of Mechanical Engineering, National Chiao Tung University, Hsinchu, Taiwan, R.O.C.

(*Received* 26 *November* 1996 *and in final form* 13 *August* 1997)

Abstract—Flow stabilization by cavity rotation in convection of air ($Pr = 0.7$) in a vertical circular cylinder heated from below is studied experimentally. The cylinder is rotated at a constant speed about its own axis. In the experiment the time variations of the air temperature at selected locations in the cylinder are measured. Results are obtained for a cylinder with diameter $D = 5$ cm, height $H = 10$ cm, imposed temperature difference $\Delta T = 5$°C to 15°C and rotation rate Ω from 0 to 346.1 rpm. The experimental data clearly show the stabilization of the thermal buoyancy driven irregular flow by the cavity rotation when the rotation rate is in certain ranges. For a given ΔT two different ranges of Ω exist for the flow to be stabilized. Outside these ranges the flow oscillates periodically or quasi-periodically in time. At given ΔT and Ω the temperature oscillation at various locations exhibits some change in amplitude but negligible change in frequency. However, change of the oscillation frequency with the rotation rate is nonmonotonic and is rather significant at high rotation rates. But this frequency change with the imposed temperature difference is small. © 1998 Elsevier Science Ltd. All rights reserved.

1. INTRODUCTION

In recent years there has been a growing interest in improving quality of bulk single-crystals often used as substrates on which various microelectronic circuits are fabricated. The crystals are normally grown by solidifying their impure liquid melts. Thus the quality of the crystals depends heavily on the buoyancy induced transport processes in the liquid melts, particularly in the vicinity of the melt-crystal interface. The unsteady heat transfer rate at the growing interface resulting from unstable temperature field driven by high thermal buoyancy will cause striations in the crystal. In addition, spatially nonuniform heat transfer rate on the interface will result in a curved interface. Control of thermal boundary conditions on crucibles and/or use of crucible rotation to produce a stable and uniform heat transfer rate at the interface are most desirable. This study intends to explore how the crucible rotation affects the temporal characteristics of the buoyancy driven flow in a bottom heated vertical circular cylinder by mainly measuring time variation of fluid temperature at various rotation rates.

In the literature considerable attention has been paid to the flow in a bottom heated vertical closed circular cylinder rotating about its own axis. Experiments for silicone oil carried out by Hudson and his coworkers [1, 2] indicate that Nusselt number increases with rotation rate. Steady axisymmetric numerical simulation was carried out by Chew [3]. The onset of steady natural convection in the cylinder was shown by Buell and Catton [4] to be rather sensitive to the lateral thermal boundary condition. Pfotenhauer *et al.* [5] reported experimental results for the effects of the cylinder geometry and rotation on the onset of convection for the low temperature liquid helium. Both the Rayleigh number associated with the convective onset and the convection heat transfer were found to depend on the rotation rate and aspect ratio of the cell. For water subject to the thermal Rayleigh number Ra $(=\beta g \Delta T D^3/\alpha\nu)$ ranging from 10^6 to 2×10^{11} and Taylor number Ta $(=\Omega^2 D^4/\nu^2)$ from 10^6 to 10^{12}, Boubnov and Golitsyn [6] experimentally observed a ring pattern of convective flow resulting from the fluid spin-up and vortex interactions between two adjacent vortices. Kirdyashkin and Distanov [7] found that a periodically changing rotation speed can result in periodical temperature changes throughout the entire liquid layer. Asymmetric convection in a vertical cylinder was experimentally found to result from lack of the azimuthal symmetry in the imposed wall temperature by Pulicani *et al.* [8]. Use of appropriate temperature gradients was experimentally demonstrated to produce a flat interface in the vertical Bridgman growth by Feigelson and Route [9]. Control of furnace temperature profile near the melt-solid interface was noted to be most effective in producing a flat interface [10]. A mathematical analysis of cen-

† Author to whom correspondence should be addressed.

NOMENCLATURE

D	diameter of cylinder
f	frequency
$f1$	first fundamental frequency
g	magnitude of the gravitational acceleration
H	height of cylinder
Pr	Prandtl number
PSD	power spectrum density
Ra	Rayleigh number, $\beta g \Delta T D^3/\alpha v$
Ra_Ω	rotational Rayleigh number, $\beta \Omega^2 \Delta T D^4/v\alpha$
t	time
T	local temperature
Ta	Taylor number, $\Omega^2 D^4/v^2$
T_H, T_L	temperatures of hot and cold walls
r, ϕ, z	dimensional cylindrical coordinates
R, Φ, Z	dimensionless cylindrical coordinates scaled with D.

Greek symbols

α	thermal diffusivity
β	thermal expansion coefficient
ΔT	temperature difference between hot and cold walls, $T_H - T_L$
Θ	dimensionless temperature $(T-T_L)/(T_H-T_L)$
Θ_{av}	nondimensional time-averaged temperature
$\overline{(\Theta-\Theta_{av})^2}$	nondimensional time-average energy of temperature fluctuation
v	kinematic viscosity
τ	dimensionless time, $t/(D^2/\alpha)$
Ω	magnitude of rotating rate.

trifugally driven thermal convection in a cylinder rotating about its own vertical axis was carried out by Homsy and Hudson [11].

Visualization of a flow of silicone oil with $Pr = 10^5$ in a vertical cylinder heated from below revealed axisymmetric flow at slightly supercritical Rayleigh number and two distinct three-dimensional flow motions at increasing Rayleigh numbers [12]. Various routes for transition from steady laminar flow to unsteady chaotic flow were experimentally determined by Rosenberger and his colleagues [13, 14] for Xenon gas in a bottom heated vertical cylinder. Both the Rule-Taken and period-doubling routes were reported for different ranges of the Rayleigh number. Similar experimental study was conducted by Kamotani *et al.* [15] for gallium melt ($Pr = 0.027$) for both vertical and inclined cylinders. Based on the temperature data various convection flow patterns were inferred.

Another geometry of considerable interest is convection in a bottom heated, infinitely bounded horizontal layer of fluid rotating at a constant angular speed about a vertical axis [16–22]. From linear stability analysis, Niller and Bisshopp [16] noted that in the limit of large Taylor number the viscous effects play an important role in a thin layer near the boundary and the critical Rayleigh number Ra_c for the onset of convection is independent of whether the boundaries are rigid or free. Numerical analysis conducted by Veronis [17] indicated that the Prandtl number exhibits significant effects on the flow and thermal structures. For the limit of infinite Prandtl number Küppers and Lortz [18] showed that no stable steady-state convective flow exists if the Taylor number exceeds certain critical value. Rossby [19] experimentally observed the subcritical instability in a water layer for $Ta > 5 \times 10^4$ and in a mercury layer for $Ta < 10^5$. In addition, for water at $Ra > 10^4$ the Nusselt number was found to increase with the Taylor number. The opposite trend is the case for mercury. Besides, at large Taylor number oscillatory convection is preferred in mercury. Based on the mean-field approximation, Hunter and Riahi [20] analytically showed the nonmonotonic variation of the Nusselt number with the Taylor number. Linear stability analysis from Rudraiah and Chandna [21] indicated that the critical Rayleigh number was relatively sensitive to the method and rate of heating. Coriolis force and the nature of the bounding surfaces of the fluid layer. The analysis from Clever and Busse [22] suggests that the critical Rayleigh number for the onset of oscillatory motion increases with the Taylor and Prandtl numbers.

Experimental data for the Nusselt number in a top heated horizontal rectangular cavity of silicone oil rotating about a vertical axis passing through the geometric center of the cavity were presented by Abell and Hudson [23]. Hathaway and Somerville [24] conducted a numerical simulation of an inclined rotating layer with the rotation vector tilted from the vertical. The tilting of the rotation vector was found to produce significant change in the flow structure. A combined theoretical, numerical and experimental study was presented by Bühler and Oertel [25] to investigate thermal convection in a rotating rectangular shallow box heated from below. First, linear stability analysis was used to predict the onset of steady and oscillatory convection and three-dimensional flow configuration. Then, numerical analysis predicted change of roll orientation with the Taylor number. Finally, flow structures at various Rayleigh and Taylor numbers

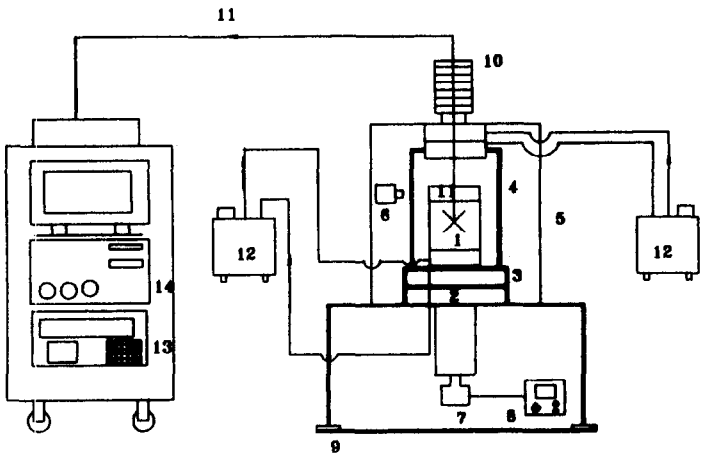

1 : test section
2 : fluid slip ring
3 : supporting frame
4 : rotating frame
5 : statatic frame
6 : photo - electric tachometer
7 : 2 Hp induction motor
8 : inverter
9 : platform
10 : slip ring
11 : thermocouples
12 : thermostat
13 : data acquisition system
14 : P.C. computer

Fig. 1. Schematic diagram of experimental system.

were visualized. Unusual flow circulation was experimentally observed by Condie and Griffiths [26] for a horizontal layer of water.

The above literature review indicates that the previous studies mainly focused on the effects of the rotation on the onset of convection and the overall heat transfer at supercritical Rayleigh numbers. The processes on how the rotation affects the flow stability and unsteady thermal characteristics are still not well understood. An experimental study was carried out here to enhance our understanding on the relation between the flow stability and cylinder rotation in convection of air in a bottom heated, vertical cylinder rotating about its own axis. Attention was focused on the ranges of the rotation rate in which rotation induced stabilization of the thermal buoyancy driven unstable flow can be obtained.

2. EXPERIMENTAL APPARATUS FOR THE TEMPERATURE MEASUREMENT

The experimental system for measuring the thermal characteristics in convection of air in a rotating vertical circular cylinder, schematically shown in Fig. 1, consists of four parts—rotating frame, test section, temperature control unit and temperature measuring unit. Figure 2 shows the details of the test section in the rotating assembly. Specifically, the cylindrical cavity of air is rotated at a constant angular speed Ω about its own axis.

The rotating frame is made up of a rotary table of 31.5 cm in diameter and is mounted on a steel shaft of 3 cm in diameter. The frame is designed to provide a space of 27.6 cm in diameter and 27.3 cm in height for housing the test section. The shaft is rotated by a two horse power d.c. motor with its speed controlled by an inverter. Besides, the rotating speed is detected by a photo-electric tachometer. Care is taken to ensure the table to rotate centrally and steadily.

The test section fixed on the rotating table is an air-containing circular cylinder of 10 cm in height and 5 cm in diameter. The top and bottom of the cylinder are both made of two 2 mm thick copper plates with 8 mm thick OMEGABOND OB-101 epoxy sandwiched between them (Fig. 3) and are controlled at uniform but different temperatures by circulating constant temperature water through them. Two fluid sliprings are used to allow the water to pass from stationary thermostats to the rotating cavity. The thermostats used are the LAUDA RK-20 compact constant temperature baths with a temperature range of $-40°C$ to $150°C$ and a resolution of $0.1°C$. Care must be taken to prevent water leak from the fluid sliprings. The side wall of the cylinder is made of 5 mm thick acrylic plates and is thermally insulated by super-lon foam. Through this arrangement the temperature uniformity of the isothermal plates can be controlled to within $\pm 0.1°C$. The sampled measured data for the temperature of the hot bottom and cold top walls at selected locations are given in Table 1.

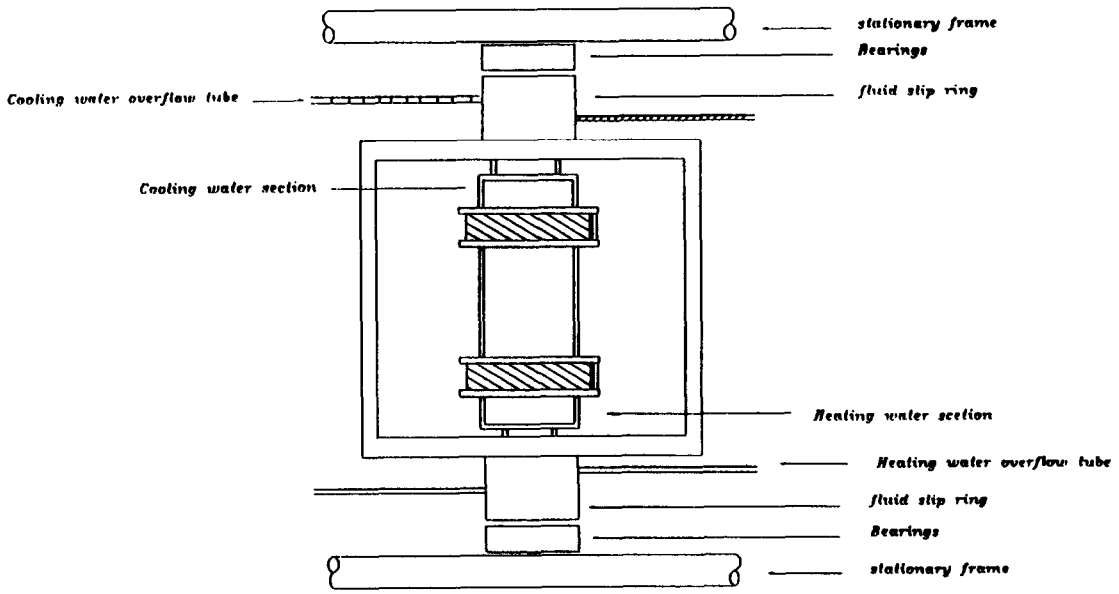

Fig. 2. Rotating assembly.

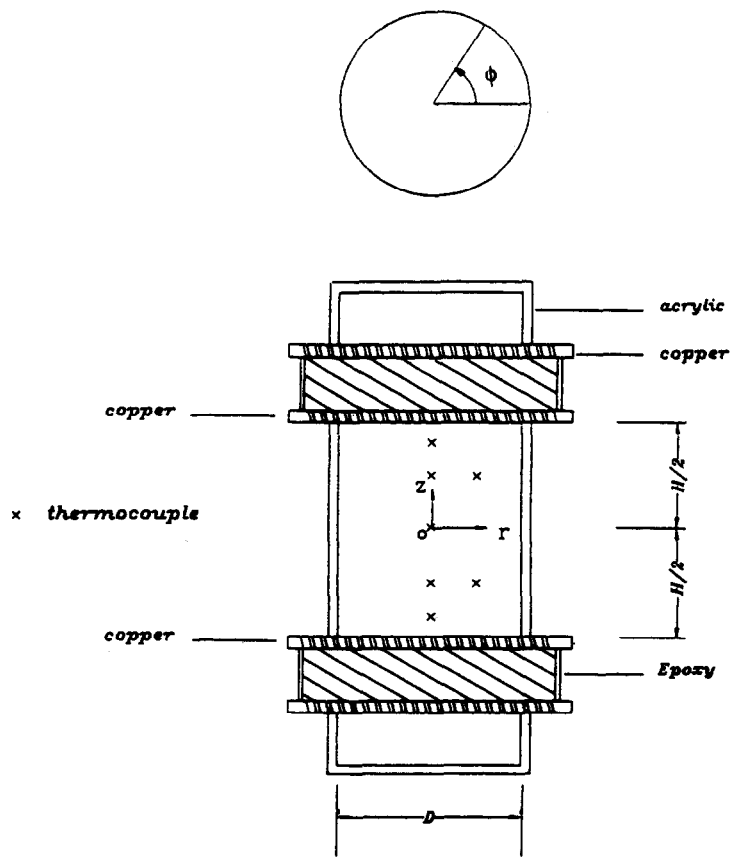

Fig. 3. Schematic diagram of the test section.

Table 1. Temperature uniformity in isothermal walls for $\Omega = 0$ rpm

Location (R, Φ)	T_L (°C)	Location (R, Φ)	T_H (°C)
0.4, 0.0	15.04	0.4, 0.0	34.97
0.4, 0.5π	14.96	0.4, 0.5π	35.04
0.4, π	15.02	0.4, π	35.04
0.4, 1.5π	15.00	0.4, 1.5π	34.99
0.0, 0.0	14.98	0.0, 0.0	35.03
0.25, 0.25π	14.96	0.25, 0.25π	35.00
0.25, 0.75π	14.99	0.25, 0.75π	35.05
0.25, 1.25π	15.04	0.25, 1.25π	34.98
0.25, 1.75π	15.01	0.25, 1.75π	34.97

For temperature measurement thermocouple connections are carefully arranged in the rotating cylinder. In particular, seven T-type thermocouples are fixed at the designated locations (Fig. 3) by high performance fine Neoflon threads, which are in turn fixed on the side wall of the cylinder and pass through the axis of the cylinder. Prior to installation the thermocouples were calibrated by the LAUDA thermostats and high precision liquid-in-glass thermometers. The voltage signals from the thermocouples were passed through a slip ring to the HP 3852A data acquisition/control system with a personal computer for further data processing. Data collection is normally started when the flow already reaches steady or statistically stable state. In view of the low speed flow encountered in the rotating cavity, velocity measurement is difficult and is not conducted here.

Test was started by first setting the thermostats at the predetermined temperatures and then recirculating the water through the top and bottom of the rotating cylinder. The mean value of the hot and cold plate temperatures is adjusted to be approximately equal to the ambient temperature, so that heat loss from the cavity to the ambient can be reduced and thermal radiation across the plates is minimized. In the meantime the cavity was rotated at the predetermined speed. Then the temperature of the air inside the cavity was measured at selected locations. After the transient stage has elapsed, data for the steady or statistically stable state were stored and analyzed. The repeatability of the experimental data was good when the initial condition of the test was controlled at the same state.

The ranges of the governing parameters to be investigated are as follows: the rotating speed varied from 0 to 346.1 rpm and the temperature difference across the cavity from 5°C to 15°C for a vertical cylinder of height $H = 10$ cm and diameter $D = 5$ cm. The results from uncertainty analysis of the measurement based on the accuracy of the measuring devices are summarized in Table 2.

3. RESULTS AND DISCUSSION

In the following only a small sample of results from the present study will be presented to illustrate the thermal characteristics in a cylindrical air cavity rotating at various rotation rates and subject to various temperature differences across the top and bottom walls. The requirements which are applied to obtain steady or statistically stable state condition are as follows. First, the experiment is operated for at least 50 times of the thermal diffusion time D^2/α, which is about 100 min. Then, we ensure that the change in the time-average temperature measured from each thermocouple is less than ± 0.1°C for a period of at least 15 min. Note that the governing nondimensional groups for the present problem are the Prandtl number Pr, thermal Rayleigh number Ra, Taylor number Ta, rotational Rayleigh number Ra_Ω and the aspect ratio of the cylinder. In the present study Pr is fixed at 0.7 and the aspect ratio at two with Ra varying from 5.89×10^4 to 1.77×10^5, Ra_Ω from 0 to 1.18×10^6 and Ta from 0 to 3.65×10^7.

3.1. *Effects of rotation on time-average temperature*

To investigate the influences of cavity rotation on the thermal characteristics of the air flow in the rotating cylinder, the time-average air temperature variations with the axial coordinate Z $(=z/D)$ along the cylinder axis were measured first at different rotation rates Ω and temperature differences ΔT. The coordinate system is chosen to rotate with the cavity with its origin at the geometric center of the cavity, as indicated in Fig. 3. Typical data from this test are exemplified in Fig. 4(a) and (b) for $\Delta T = 10$°C at increasing Ω. The corresponding thermal Rayleigh number Ra is 1.17×10^5. It is noted from these data that in a nonrotating cylinder ($\Omega = 0$) large temperature gradients exist in the regions near the top and bottom of the cavity (Fig. 4(a)). Outside these thermal boundary layers in the cavity core the flow is nearly isothermal. This unique temperature distribution obviously results from the thermal buoyancy driven boundary layer flow in the stationary cavity at this high thermal Rayleigh number [28]. As the cylinder rotates at 30.8 rpm the temperature gradients near the horizontal plates are significantly reduced and in the cavity core the temperature is almost lin-

Table 2. Summary of uncertainty analysis

Parameters	Uncertainty
H and D (m)	± 0.00025 m
T_H, T_L	± 0.1°C (non-rotating)
T_H, T_L	± 0.2°C (rotating)
T (thermocouples)	± 0.05°C
α (m^2/s)	$\pm 0.07\%$
β (K^{-1})	$\pm 0.05\%$
ρ (kg/m^3)	$\pm 0.05\%$
ν (m^2/s)	$\pm 0.07\%$
Ω (rpm)	$\pm 0.3\%$
Ta	$\pm 10.5\%$
Ra	$\pm 8.5\%$
Ra_Ω	$\pm 11.5\%$

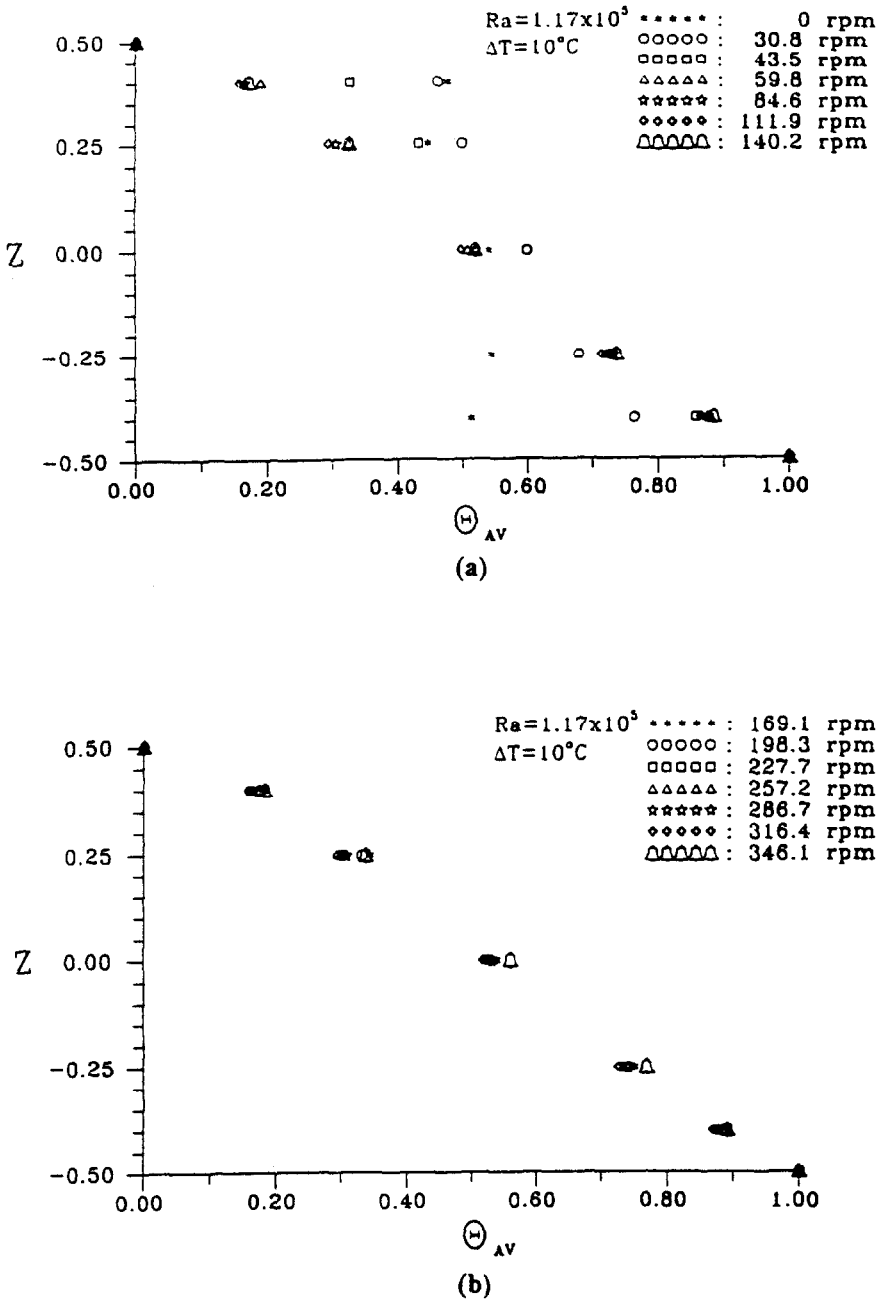

Fig. 4. Nondimensional time-average temperature distribution along Z-axis at $\Delta T = 10°C$ ($Ra = 1.17 \times 10^5$) for different rotation rates: (a) 0–140.2 rpm, and (b) 169.1–346.1 rpm.

early distributed in the vertical direction. This trend continues as the rotation rate is further raised. For $\Omega \geqslant 59.8$ rpm no thermal boundary layer exists in the cavity and the air temperature varies nearly linearly from the hot bottom plate to the cold top plate. This conduction-like temperature distribution is conjectured to result from the suppression of the thermal buoyancy driven flow by the Coriolis force associated with the cavity rotation, as noted in our previous numerical simulation [29] for a rotating cubic air cavity. It is also noted that for a larger temperature difference ΔT across the horizontal plates a higher rotation rate is required to suppress the flow.

3.2. *Rotation induced flow transition*

The rotation induced flow transition among the steady, time periodic, quasi-periodic and chaotic states in the differentially heated cylinder is then investigated by examining the time variations of the measured instantaneous air temperature at selected

locations in the cavity. Only the long term results are studied at which the temperature already reaches steady or statistically stable state. Attention is focused on the change of the temperature oscillation amplitude and frequency with the rotation rate.

The temporal stability of the air flow affected by the cavity rotation is first illustrated by showing the measured data in Fig. 5(a) and (b) at location $(R, \Phi, Z) = (0, 0, 0)$ for $\Delta T = 5$ and 10°C. Since only the data at the statistically stable state are recorded, the dimensionless time $\tau = 0$ stands for a certain arbitrary selected time instant at that state. The results in

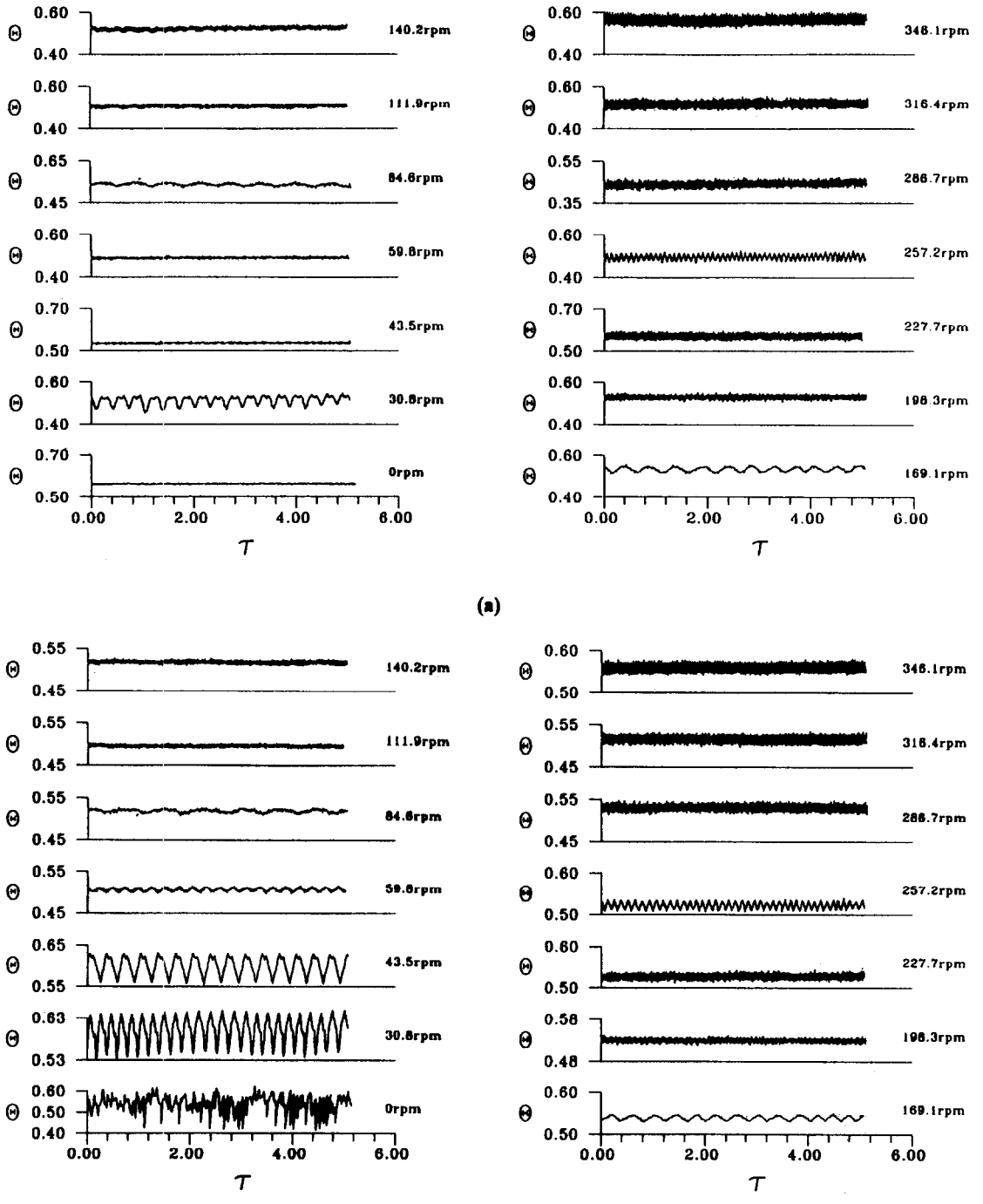

Fig. 5. Measured time records of air temperature at location $(R, \Phi, Z) = (0, 0, 0)$ for various rotation rates for (a) $\Delta T = 5$°C ($Ra = 5.89 \times 10^4$) and (b) $\Delta T = 10$°C ($Ra = 1.17 \times 10^5$).

Fig. 5(a) for $\Delta T = 5°C$ ($Ra = 5.89 \times 10^4$) at various rotation rates manifest that at $\Omega = 0$ rpm the flow is in a very small amplitude oscillation. The oscillation amplitude is less than 0.01 in a dimensionless unit or less than 0.05°C dimensionally. This small amplitude oscillation can be considered as resulting from the background noise always existing in the test apparatus, and the flow can be regarded as steady. As the cylinder is rotated at 30.8 rpm the flow is in a large amplitude, low frequency time periodic oscillation. Thus the flow experiences a Hopf bifurcation, a transition from a steady to a time periodic state, for a raise of Ω from 0 to 30.8 rpm. It is of interest to note that for a further increase of Ω to 43.5 and 59.8 rpm the flow is stabilized and is in a small amplitude oscillation. The oscillation amplitude is all less than 0.1°C and hence the flow is essentially steady. Therefore a reverse Hopf bifurcation occurs for Ω raising from 30.8 to 43.5 rpm. At a higher Ω of 84.6 rpm the flow exhibits a discernible low frequency low amplitude oscillation with an even smaller amplitude high frequency oscillation superimposed on it. At slightly higher rotation rates of 111.9 and 140.2 rpm the high frequency component grows significantly in amplitude. However, at a still higher Ω of 169.1 rpm the high frequency component is suppressed again and the flow is dominated by the low frequency large amplitude oscillation. This trend of the nonmonotonic change of the frequency content of the temperature oscillation with the rotation rate continues when Ω is raised further. Note that for 198.3 rpm $\leqslant \Omega \leqslant$ 346.1 rpm the oscillation amplitude increases slightly with the rotation rate.

When the cylinder is subject to a much larger temperature difference $\Delta T = 10°C$ ($Ra = 1.17 \times 10^5$) the thermal buoyancy is so high that the induced flow is in a large amplitude chaotic oscillation as the cavity is stationary ($\Omega = 0$), as evident from the data in Fig. 5(b). The flow becomes time periodic but still in a large amplitude oscillation when the cylinder rotates at 30.8 rpm. At a slightly higher Ω of 43.5 rpm the flow remains time periodic but oscillates in a smaller amplitude and at a lower frequency. Substantial reduction in the oscillation amplitude occurs when Ω is raised to 59.8 and 84.6 rpm. As the cylinder rotates at 111.9 and 140.2 rpm the flow is dominated by a high frequency low amplitude oscillation. More specifically, the oscillation amplitude is about 0.012 dimensionlessly or 0.12°C dimensionally, which is of the same order as the background disturbances. Hence the flow can be regarded as steady. This clearly shows the flow stabilization by the cavity rotation when the rotation rate is raised from 84.6 rpm to 111.9 and 140.2 rpm. When the rotation rate continues to increase from 140.2 rpm to 346.1 rpm, the flow undergoes transitions first from a steady to a time periodic state, then to a steady state (Ω = 198.3 rpm), but back to a time periodic state in a certain range of Ω, and finally to a chaotic state at a high Ω ($\geqslant$286.7 rpm). This sequence of flow transition is similar to that just discussed for the cases with $\Delta T = 5°C$.

The spatial dependence of flow oscillation is exam-

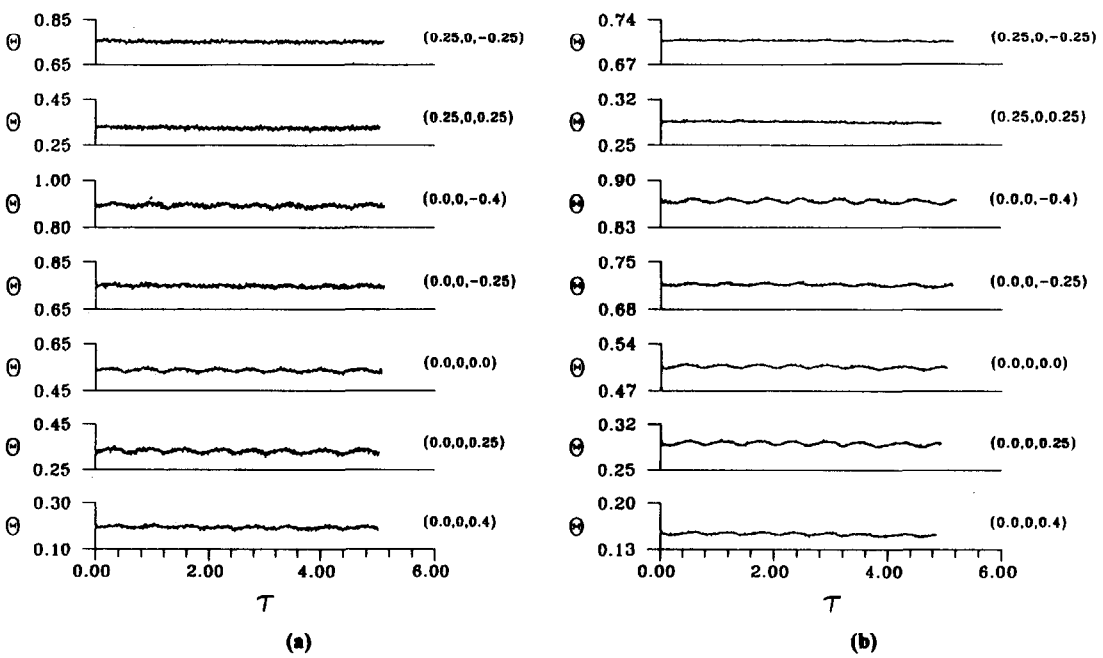

Fig. 6. Measured time histories of air temperature at various locations at $\Omega = 84.6$ rpm ($Ta = 2.175 \times 10^6$) for temperature difference (a) $\Delta T = 5°C$ ($Ra = 5.89 \times 10^4$, $Ra_\Omega = 2.35 \times 10^4$) and (b) $\Delta T = 15°C$ ($Ra = 1.77 \times 10^5$, $Ra_\Omega = 7.06 \times 10^4$).

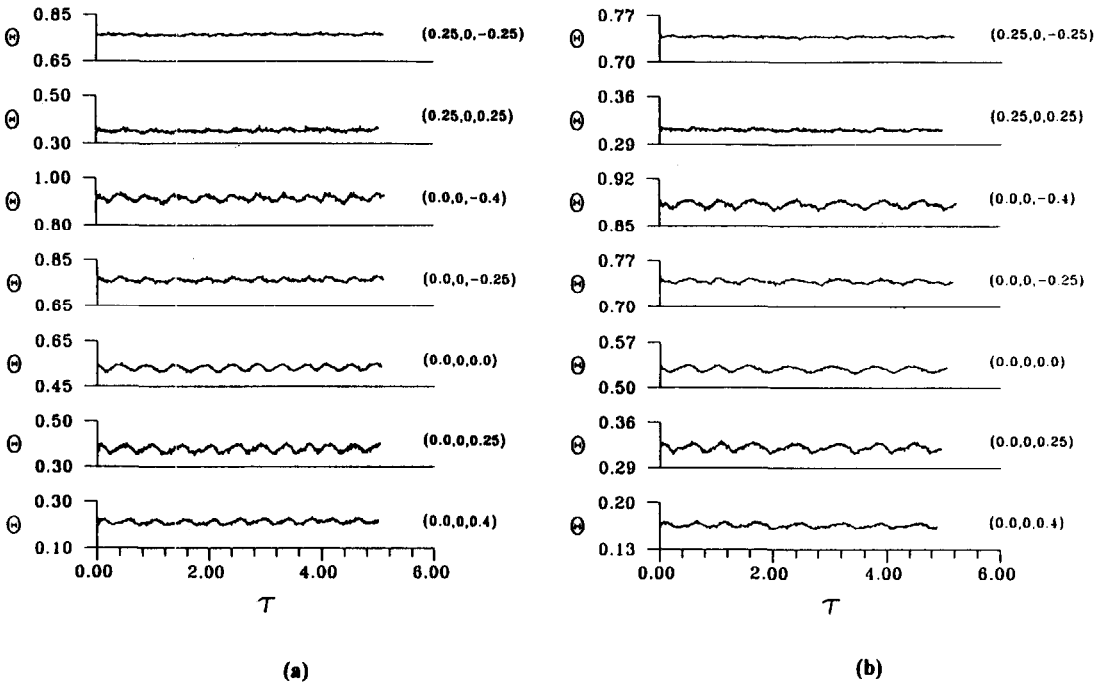

Fig. 7. Measured time histories of air temperature at various locations at $\Omega = 169.1$ rpm ($Ta = 8.71 \times 10^6$) for temperature difference (a) $\Delta T = 5°C$ ($Ra = 5.89 \times 10^4$, $Ra_\Omega = 9.42 \times 10^4$) and (b) $\Delta T = 15°C$ ($Ra = 1.77 \times 10^5$, $Ra_\Omega = 2.82 \times 10^5$).

ined next. Typical data to illustrate this dependence are shown in Figs. 6 and 7 for $\Delta T = 5$ and 15°C at two different rotation rates. The associated Ra, Ra_Ω and Ta are indicated in the figure captions. Checking these time histories at seven different locations reveals that in spite of the large change in the oscillation amplitude with space, the flow at all detected locations oscillates periodically with time at the same frequency for a given Ω. Specifically, the signals are characterized by a high frequency small amplitude oscillation superimposed on a low frequency high amplitude oscillation. Note that at the cylinder axis ($R = 0$) the flow oscillates at nearly the same amplitude. The oscillation is smaller off the axis.

3.3. *Frequency content of flow oscillation*

To further illustrate the characteristics of the flow oscillation, the power spectrum densities (PSD) of the measured time histories were obtained by a fast Fourier Transform analysis. The results in Fig. 8(a)–(c) for $\Delta T = 5$, 10 and 15°C at location (0, 0, 0) for various rotation rates indicate that the effects of the thermal buoyancy (temperature difference) on the oscillation frequency are small, as evident from the comparison of the corresponding plots at the same Ω for different ΔT. However, the change in the oscillation amplitude (the value of PSD) with the temperature difference and rotation rate is noticeable. Normally the dimensional oscillation amplitude increases with ΔT. But this increase in the temperature oscillation amplitude is less than that in the imposed ΔT. Examining the results in Fig. 8(a) for $\Delta T = 5°C$ discloses that at $\Omega = 0$ rpm the power spectrum density is rather small and no frequency peak exists, indicating the flow being in a very small amplitude random oscillation and being regarded as steady. At a lower rotation rate of 30.8 rpm the temperature oscillation is dominated by a single fundamental frequency $f1 = 0.030$ and one harmonics at 0.060. For slightly higher Ω of 43.5 and 59.8 rpm the PSD value are low and the flow is regarded as steady as just discussed. The temperature oscillation is characterized by an even lower frequency of 0.017 at 84.6 rpm. A significant increase in the oscillation frequency occur for Ω raised to 111.9 and 140.2 rpm. However large drop in the oscillation frequency ensues for a rise of Ω to 169.1 rpm, followed by a big increase in the frequency for a further rise of Ω to 198.3 rpm. Then there is a gradual reduction in the oscillation frequency with the rotation rate for Ω up to 257.2 rpm. But as Ω is raised to 286.7 rpm, the frequency again increases drastically. Beyond that the frequency again drops gradually. The above results clearly show the complex variation of the oscillation frequency with the rotation rate. Similar characteristics in the change of the dominant oscillation frequency with the rotation rate are noted in Fig. 8(b) and (c) for higher ΔT. At these higher ΔT there exists another frequency peak close to the dominant first fundamental frequency in each plot for $\Omega \geqslant 198.3$ rpm. This presence of the second fundamental frequency mode indicates that the flow is quasi-periodic [30].

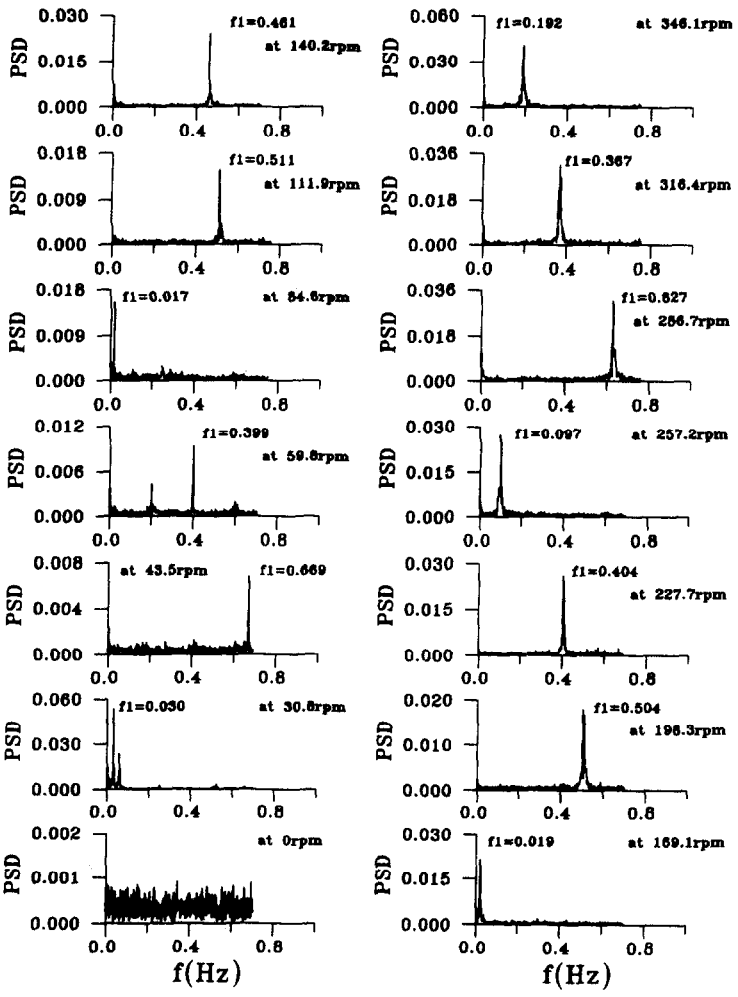

(a)

Fig. 8. Power spectrum densities of Θ for various rotation rates at location $(R, \Phi, Z) = (0, 0, 0)$ for (a) $\Delta T = 5°C$ ($Ra = 5.89 \times 10^4$), (b) $\Delta T = 10°C$ ($Ra = 1.17 \times 10^5$) and (c) $\Delta T = 15°C$ ($Ra = 1.77 \times 10^5$).

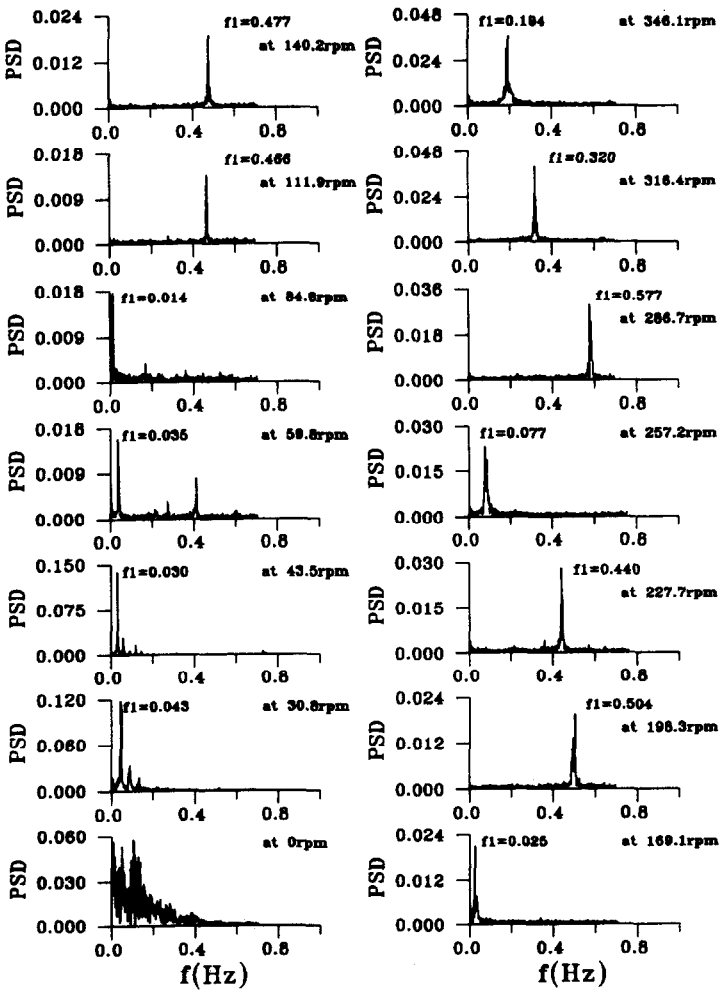
f1=0.477
at 140.2rpm
f1=0.184
at 346.1rpm
f1=0.466
at 111.9rpm
f1=0.320
at 316.4rpm
f1=0.014
at 84.6rpm
f1=0.577
at 286.7rpm
f1=0.035
at 59.6rpm
f1=0.077
at 257.2rpm
f1=0.030
at 43.5rpm
f1=0.440
at 227.7rpm
f1=0.043
at 30.6rpm
f1=0.504
at 198.3rpm
at 0rpm
f1=0.025
at 169.1rpm
PSD
f(Hz)

(b)

Fig. 8(b).

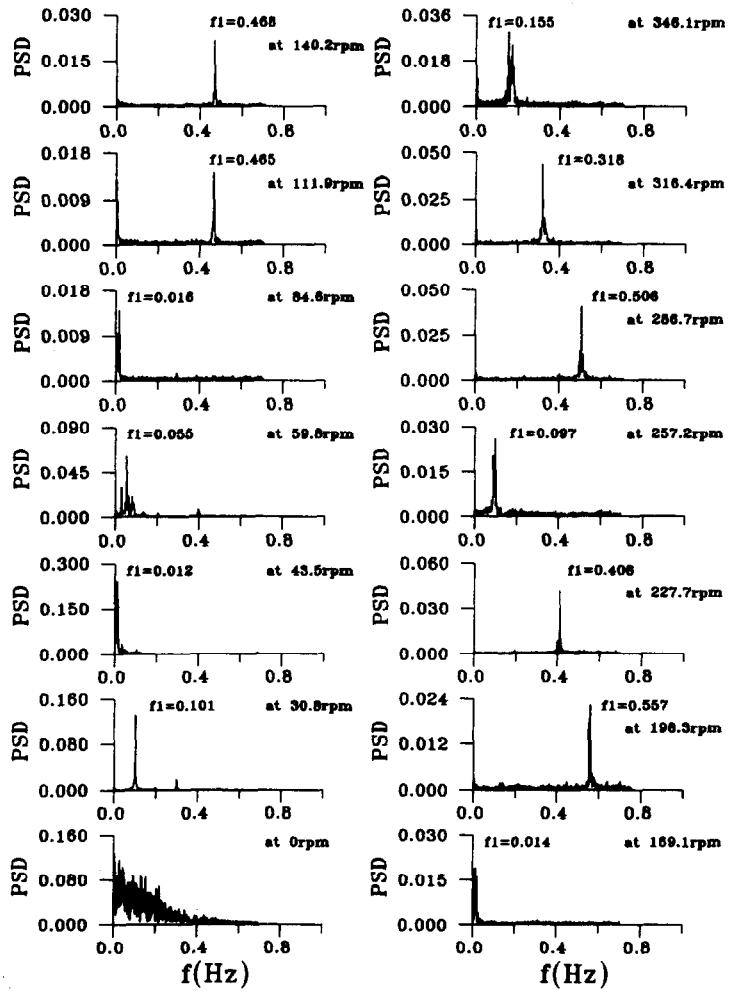
f1=0.468
at 140.2rpm
f1=0.155
at 346.1rpm
f1=0.465
at 111.9rpm
f1=0.318
at 316.4rpm
f1=0.016
at 84.6rpm
f1=0.506
at 286.7rpm
f1=0.055
at 59.8rpm
f1=0.097
at 257.2rpm
f1=0.012
at 43.5rpm
f1=0.406
at 227.7rpm
f1=0.101
at 30.8rpm
f1=0.557
at 196.3rpm
at 0rpm
f1=0.014
at 169.1rpm
PSD
f(Hz)

(c)

Fig. 8(c).

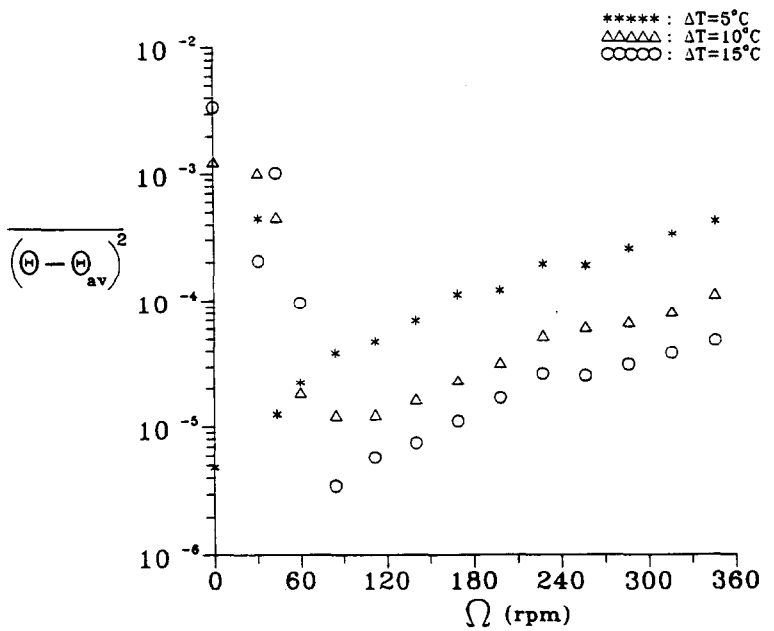

Fig. 9. Variations of time-average energy of temperature fluctuation with rotation rate at different ΔT.

3.4. *Energy of temperature oscillation*

An overall characteristic of the flow stabilization by the cavity rotation can be conveniently expressed by the time-average energy of the dimensionless air temperature function $\overline{(\Theta-\Theta_{av})^2}$. Typical results for the energy of temperature fluctuation are shown in Fig. 9 for $\Delta T = 5$, 10 and 15°C at the geometrical center of the cylinder for various Ω. The effects of the cavity rotation on the flow stability can be clearly seen from these results. Specifically, in the range of Ω from 60 to 120 rpm the fluctuation energy is small and the flow is stabilized by the cylinder rotation. Outside this range the cavity rotation does not stabilize the flow.

4. CONCLUDING REMARKS

Through a detailed experimental measurement of the time-average and instantaneous temperatures in a differentially heated, vertical, air-containing cylinder, the effects of rotation rate on the temporal stability of the flow were investigated in the present study. The data suggest that the time-average temperature distributions along the Z-axis for various rotation rates are all linear and nearly overlap as Ω exceeds a certain critical value, implying the suppression of the thermal buoyancy driven flow by the cavity rotation at a high Ω. Flow re-stabilization at increasing rotation rate characterized by the presence of the two different ranges of the rotation rates for the steady flow to prevail was clearly shown from the data for the time records of the air temperature. Moreover, for a given rotation rate the oscillation amplitude of the air temperature depends significantly on the imposed temperature difference. But the oscillation frequency is almost the same. Finally, the power spectrum density analysis of the recorded data clearly indicates that in a rotating cavity the temperature oscillation is mainly dominated by a single fundamental frequency. The variation of the frequency with the rotation rate is nonmonotonic.

During the course of this investigation it is noted that cavity rotation does have the effects of stabilizing the thermal buoyancy driven flow when Ω is in proper ranges. But the detailed physical processes through which flow transition is induced are not clear. A comprehensive numerical simulation to calculate this complicate transient transitional flow is required and will be explored in the near future. Moreover, effects of the cavity rotation on the stabilization of the liquid metal flow are particularly important in growing bulk crystals for the semiconductor industry and will be investigated in the near future.

Acknowledgement—The financial support of this study by the engineering division of National Science Council of Taiwan, Republic of China through the contract NSC 83-0401 E-009-009 is greatly appreciated.

REFERENCES

1. Hudson, J. L., Tang, D. and Abell, S., Experiments on centrifugal driven thermal convection in a rotating cylinder. *J. Fluid Mech.*, 1978, **86**, 147–159.
2. Tang, D. and Hudson, J. L., Experiments on a rotating fluid heated from below. *Int. J. Heat Mass Transfer*, 1983, **26**, 943–949.
3. Chew, J. W., Computation of convective laminar flow in rotating cavities. *J. Fluid Mech.*, 1985, **153**, 339–360.

4. Buell, J. C. and Catton, I., Effect of rotation on the stability of a bounded cylindrical layer of fluid heated from below. *Phys. Fluids*, 1983, **26,** 892–896.
5. Pfotenhauer, J. M., Niemela, J. J. and Donnelly, R. J., Stability and heat transfer of rotating cryogens. Part 3. Effects of finite cylindrical geometry and rotation on the onset of convection. *J. Fluid Mech.*, 1987, **175,** 85–96.
6. Boubnov, B. M. and Golitsyn, G. S., Experimental study of convective structures in rotating fluid. *J. Fluid Mech.*, 1986, **167,** 503–531.
7. Kirdyashkin, A. G. and Distanov, V. E., Hydrodynamics and heat transfer in a vertical cylinder exposed to perodically varying centrifugal forces (accelerated crucible rotation technique). *Int. J. Heat Mass Transfer*, 1990, **33,** 1397–1415.
8. Pulicani, J. P., Krukowski, S., Iwan, J., Alexander, D., Ouazzani, J. and Rosenberger, F., Convection in an asymmetrically heated cylinder. *Int. J. Mass Transfer*, 1992, **35,** 2119–2130.
9. Feigelson, R. S. and Route, R. K., Vertical Bridgman growth of $CdGeAs_2$ with control of interface shape and orientation. *Journal of Crystal Growth*, 1980, **49,** 261–273.
10. Dutta, P. S., Sangunni, K. S., Bhat, H. L. and Kumar, V., Growth of gallium antimonide by vertical Bridgman technique with planar crystal-melt interface. *Journal of Crystal Growth*, 1994, **141,** 44–50.
11. Homsy, G. M. and Hudson, J. L., Heat transfer in a rotating cylinder of fluid heated from above. *Int. J. Heat Mass Transfer*, 1971, **14,** 1149–1659.
12. Figliola, R. S., Convection transitions within a vertical cylinder heated from below. *Phys. Fluids*, 1986, **29,** 2028–2031.
13. Olson, J. M. and Rosenberger, F., Convective instabilities in a closed vertical cylinder heated from below. Part 1. Monocomponent gases. *J. Fluid Mech.*, 1978, **92,** 609–629.
14. Abernathey, J. R. and Rosenberger, F., Time-dependent convective instabilities in a closed vertical cylinder heated from below. *J. Fluid Mech.*, 1985, **160,** 137–154.
15. Kamotani, Y., Weng, F. B. and Ostrach, S., Oscillatory natural convection of a liquid metal in circular cylinders. *Journal of Heat Transfer*, 1994, **116,** 627–632.
16. Niller, P. P. and Bisshopps, F. E., On the influence of Coriolis force on onset of thermal convection. *J. Fluid Mech.*, 1965, **22,** 753–761.
17. Veronis, G., Large-amplitude Bënard convection in a rotating fluid. *J. Fluid Mech.*, 1968, **31,** 113–139.
18. Küppers, G. and Lortz, D., Transition from laminar convection to thermal turbulence in a rotating fluid layer. *J. Fluid Mech.*, 1969, **35,** 609–620.
19. Rossby, H. T., A study of Bënard convection with and without rotation. *J. Fluid Mech.*, 1969, **36,** 309–335.
20. Hunter, C. and Riahi, N., Nonlinear convection in a rotating fluid. *J. Fluid Mech.*, 1975, **72,** 433–454.
21. Rudraiah, N. and Chandna, O. P., Effects of Coriolis force and nonuniform temperature gradient on the Rayleigh–Bënard convection. *Can. J. Phys.*, 1986, **64,** 90–99.
22. Clever, R. M. and Busse, F. H., Nonlinear properties of convection rolls in a horizontal layer rotating about a vertical axis. *J. Fluid Mech.*, 1979, **94,** 609–627.
23. Abell, S. and Hudson, J. L., An experimental study of centrifugally driven free convection in rectangular cavity. *Int. J. Heat Mass Transfer*, 1975, **18,** 1415–1423.
24. Hathaway, D. H. and Somerville, R. C. J., Three-dimensional simulations of convection in layers with tilted rotation vectors. *J. Fluid Mech.*, 1983, **126,** 75–89.
25. Bühler, K. and Oertel, H., Thermal cellular convection in rotating rectangular boxes. *J. Fluid Mech.*, 1982, **114,** 261–282.
26. Condie, S. A. and Griffiths, R. W., Convection in rotating cavity : modeling ocean circulation. *J. Fluid Mech.*, 1989, **207,** 453–474.
27. Homsy, G. M. and Hudson, J. L., Centrifugally driven thermal convection in a rotating cylinder. *J. Fluid Mech.*, 1969, **35,** 33–52.
28. Lee, T. L. and Lin, T. F., Three-dimensional natural convection of air in an inclined cubic cavity. *Numerical Heat Transfer*, 1995, **27,** 681–703.
29. Lee, T. L. and Lin, T. F., Transient three-dimensional convection of air in a differentially heated rotating cubic cavity. *Int. J. Heat Mass Transfer*, 1996, **39,** 1243–1255.
30. Argyris, J., Faust, G. and Haase, M., An adventure in chaos. *Comp. Math. in Appl. Mech. and Eng.* 1991, **91,** 997–1091.